Journal of Applied Physics

X-ray emission from 30 J Blumlein operated compact diode

M. Zakaullah and J. Worley

Citation: J. Appl. Phys. **88**, 1251 (2000); doi: 10.1063/1.373811
View online: http://dx.doi.org/10.1063/1.373811
View Table of Contents: http://jap.aip.org/resource/1/JAPIAU/v88/i3
Published by the AIP Publishing LLC.

JOURNAL OF APPLIED PHYSICS VOLUME 88, NUMBER 3 1 AUGUST 2000

X-ray emission from 30 J Blumlein operated compact diode

M. Zakaullah[a)] and J. Worley[b)]
Department of Physics, Quaid-i-Azam University 45320 Islamabad, Pakistan

(Received 23 September 1999; accepted for publication 26 April 2000)

An x-ray emitting diode of impedance 2.3 Ω with a knife-edge cathode energized by a 90 kV, 30 J, solid dielectric Blumlein driver of pulse length 10 ns is studied. X-ray emission from titanium, copper, molybdenum, tin, tantalum, and lead anodes was investigated. The radiation yield from titanium and copper is low. Molybdenum and tin emit a significant part as K_α line radiation, whereas the emission with tantalum and lead anode is essentially continuum radiation. The ratio of line to continuum with molybdenum target is estimated 17%±10%. © *2000 American Institute of Physics.* [S0021-8979(00)03015-2]

I. INTRODUCTION

There has been considerable interest in sub-microsecond and nanosecond pulsed x-ray sources for possible uses in radiography, crystallography, x-ray contact microscopy, and x-ray backlighting. The pulsed plasmas, for example, *X* pinches,[1] vacuum sparks,[2] *Z* pinches,[3] and plasma focus[4,5] are among the other sources being developed. However, electron bombardment of solid targets is still among the most important practical methods of generating x-rays.[6,7] The latter technique is commonly used in conventional x-ray tubes. The electrons emitted thermionically, are accelerated by an appropriate potential and directed to some target. One may also attempt to operate an x-ray emitting diode which employs field emission instead of thermionic emission. The Compact Electron Radiation Emission Source (CERES) operated by a Blumlein-type driver is such an example.

II. EXPERIMENTAL SETUP

CERES uses an arrangement of three Blumleins[8] to produce a short 90 kV pulse at the diode. The Blumleins are charged in parallel, but discharged in series. The actual arrangement is shown in Fig. 1. The Blumleins share a common trigger gap, which has a very low inductance. When triggered, each line produces a pulse of 30 kV at the far end from the trigger. Transit time isolation enables the three to be connected in series, which works for the period of the output pulse. The length of the output pulse is twice the electrical length of the lines. Each half of each line has a capacitance of 11 nF, so that with a charging voltage of 30 kV the total stored energy is 30 J. The impedance of each half of each Blumlein is about 0.75 Ω, so each Blumlein has an output impedance of 1.5 Ω, and the final output impedance is about 4.5 Ω. The maximum current into the diode has been measured as 26 kA at a voltage of 70 kV. To ensure very low inductance the trigger gap is constructed as a continuation of the parallel plate lines. A pointed plunger pierces a thin Mylar sheet between foil electrodes. The Mylar and a small area of the electrodes is renewed between shots. A small electromagnet is used to drop the plunger. This successful but unsophisticated arrangement could probably be replaced by a parallel plate triggertron to get synchronization with other equipment. The inductance of the gap needs to be about 1 nH so the gap would need to be very small. The diode consists of a knife-edged cathode which is a replaceable piece of razor blade and a flat plate anode. Different metal foils, for example, titanium, copper, molybdenum, tin, tantalum, and lead were mounted at the anode in this experiment. The anode materials, their atomic number (*Z*), and respective K_α absorption edges are summarized in Table I. The CERES electrodes are enclosed in a small conical shaped, round vacuum chamber made of about 3.5-mm-thick Perspex, which is covered by 100-μm-thick aluminum foil, stuck to its surface. This is to provide a low inductance current path. At one side, about 2 cm diameter seat is engraved at the chamber surface, leaving the chamber wall thickness about 1.5 mm. This window was used either to record x-ray pulse wave form by a Quantrad *p-i-n* diode which has a 100 mm^2 active area, with 250 μm thick active layer, or the Ross filter set pair along with Kodak x-ray direct exposure film (DEF). A Philips photomultiplier tube (PMT) optically coupled with 25-mm-thick plastic scintillator NE 102A was used to record the temporal wave form of emitted hard x rays, which also serves as a check for the reproducibility of the system. A rotary vane pump was used to evacuate the system to 10^{-2} mbar, which is found adequate in this experiment. When the output pulse is delivered to the diode, electrons are emitted from the knife-edge cathode and accelerated to a flat-plate anode.

To analyze the *X* radiation, whether dominantly continuum, or containing a significant part of the line radiation characteristic of the target, three sets of Ross filter pairs, (22 μm Cu, 10 μm Mo), (50 μm Mo, 6 μm Ta) and (12 μm Ta, 12.5 μm Pb) are used with Mo, Ta, and Pb targets, respectively. The transmission characteristics of the filter set (22 μm Cu, 10 μm Mo) is given in Fig. 2. A resistive divider with attenuation factor of 400, is connected across the diode. The voltage pulse from the divider is further attenuated 10× at the oscilloscope end. This pulse serves as a monitor of

[a)]Electronic mail: zaka_qau_pk@yahoo.com
[b)]Present address: The Blackett Laboratory, Imperial College of Science Technology & Medicine, Prince Consort Road, London SW7 2BZ UK.

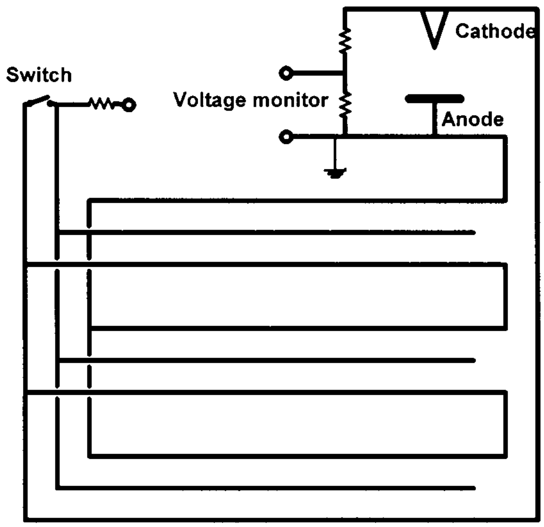

FIG. 1. Schematic arrangement of Blumleinns and compact x-ray emitting diode.

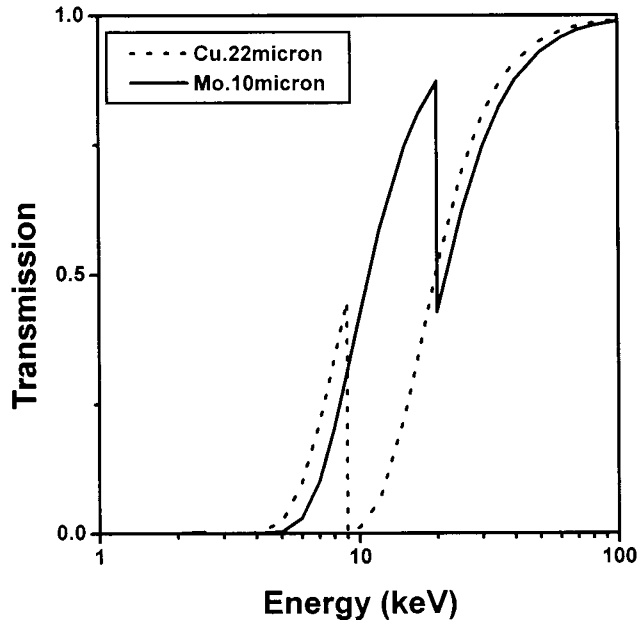

FIG. 2. Transmission characteristics of the Ross-filter set used in the experiment.

voltage appearing across the diode and is also used to externally trigger the oscilloscope. A four channel, 100 MHz GOULD oscilloscope is used to record electrical signals.

III. RESULTS

The appropriate separation between anode and cathode for high x-ray emission is found to be 1.3 mm. Different widths of the razor blade as a knife-edge cathode were tried and 3.5 mm was found most appropriate in this experiment. From the electron beam induced damage on the target foil, one may estimate the peak electron current density as follows: One may consider the dimensions of damage on the target as estimate of the electron beam cross section. The ratio of peak discharge current to beam cross section gives us the peak electron current density, which is found to be 6 ± 0.5 MA/cm^2. The optimum width of the razor blade corresponds to optimum current density for high x-ray generating efficiency in this system. The *p*-*i*-*n* diode was mounted at the 1.5-mm-thick Perspex window and was further masked with 25 μm Be and 12 μm Mylar. In this arrangement, the diode may detect photons of energy greater than 5 keV, it has the highest detection efficiency around 10 keV which remained appreciable up to 40 keV. Its response curve is depicted in Fig. 3. The voltage pulse which appears across the diode is quite narrow, of width [full width at half maximum (FWHM)] $\sim$10 ns. The x-ray photons which may pass through the chamber wall and PMT shield have an energy exceeding 25 keV. In some shots, the PMT was shielded by an additional 1.5 mm Pb or 15.8 mm Al. The 1.5 mm Pb filter has a weak transmission band at 88 keV and allows effective transmission of photons with energy exceeding 150 keV. When the PMT was shielded with 1.5-mm-thick lead, the signal became very weak and the signal to noise ratio was hopeless. The 15.8 mm Al plate along with 5 mm Al PMT shield allows us to detect photons exceeding 50 keV. The PMT signal is found to be delayed by about 40 ns, whereas the *p*-*i*-*n*-diode signal is almost synchronized with the HV probe signal. It is resolved that the delay in the PMT signal is introduced due to internal transit time of the detector; otherwise, the x-ray emission is almost coincident with

TABLE I. K_α absorption edges of different target materials used in the experiment.

Anode	Z	K_α (keV)
Ti	22	4.96
Cu	29	8.98
Mo	42	20.00
Sn	50	29.19
Ta	73	67.4
Pb	82	88.00

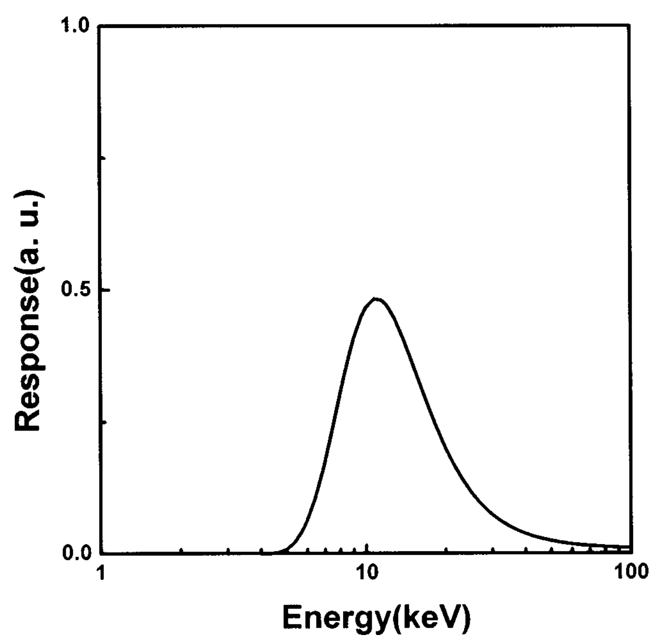

FIG. 3. Response curve of the *p*-*i*-*n* diode in the experimental arrangement, absorption effects of chamber wall, and light tight filter are encountered.

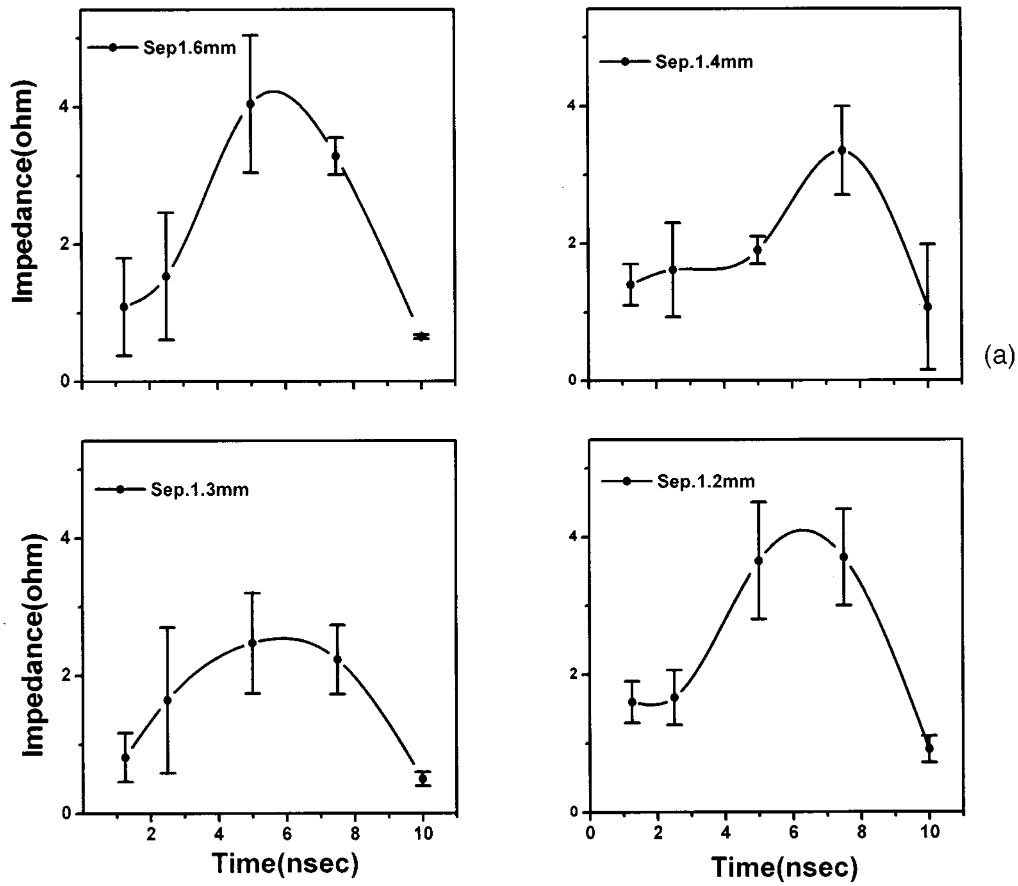

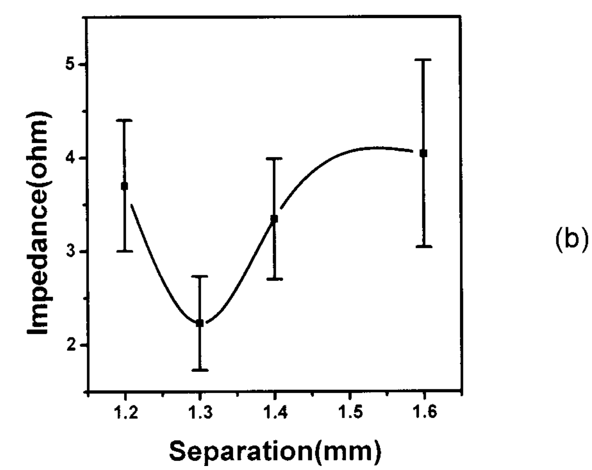

FIG. 4. (a) Temporal variation of diode impedance for different separations of anode and cathode. (b) Variation of maximum diode's impedance with electrodes' separation.

the application of high voltage across the diode. The pulse width (FWHM) of the *p*-*i*-*n*-diode signal is 10 ± 1 ns, whereas the pulse width (FWHM) of the PMT signal is found to be 20 ± 2 ns. The difference was found to be due to the PMT being saturated. When the PMT was shielded with 15.8-mm-thick aluminum, the pulse width of the PMT reduced to 10 ± 1 ns, and the pulse width of the two detectors coincide. It is interesting to note that with different targets, although the amplitude of the x-ray pulses is changed, no noticeable change in pulse width or temporal synchronization of x-ray emission relative to HV pulse is recorded.

The x-ray emission is found very reproducible in the case of a lead target, not affected even by the target foil damage, which is observed after few shots. The tantalum and tin targets also generate quite reproducible x-ray emission, which is slightly degraded with the target damage. In the case of a molybdenum target, although the emission is reproducible, degradation with target damage is significant. With copper and titanium targets, the amplitude is lowered to 60%–70% of the value for Pb. For these two target materials, the recording of images on x-ray film was not very successful. Probably the energy of the photons as well as the radiation intensity is lower, and a significant number of photons could not get through the chamber wall. For titanium, copper, molybdenum, and tin targets, a copper mesh is also imaged on DEF. Clear and well defined images are formed

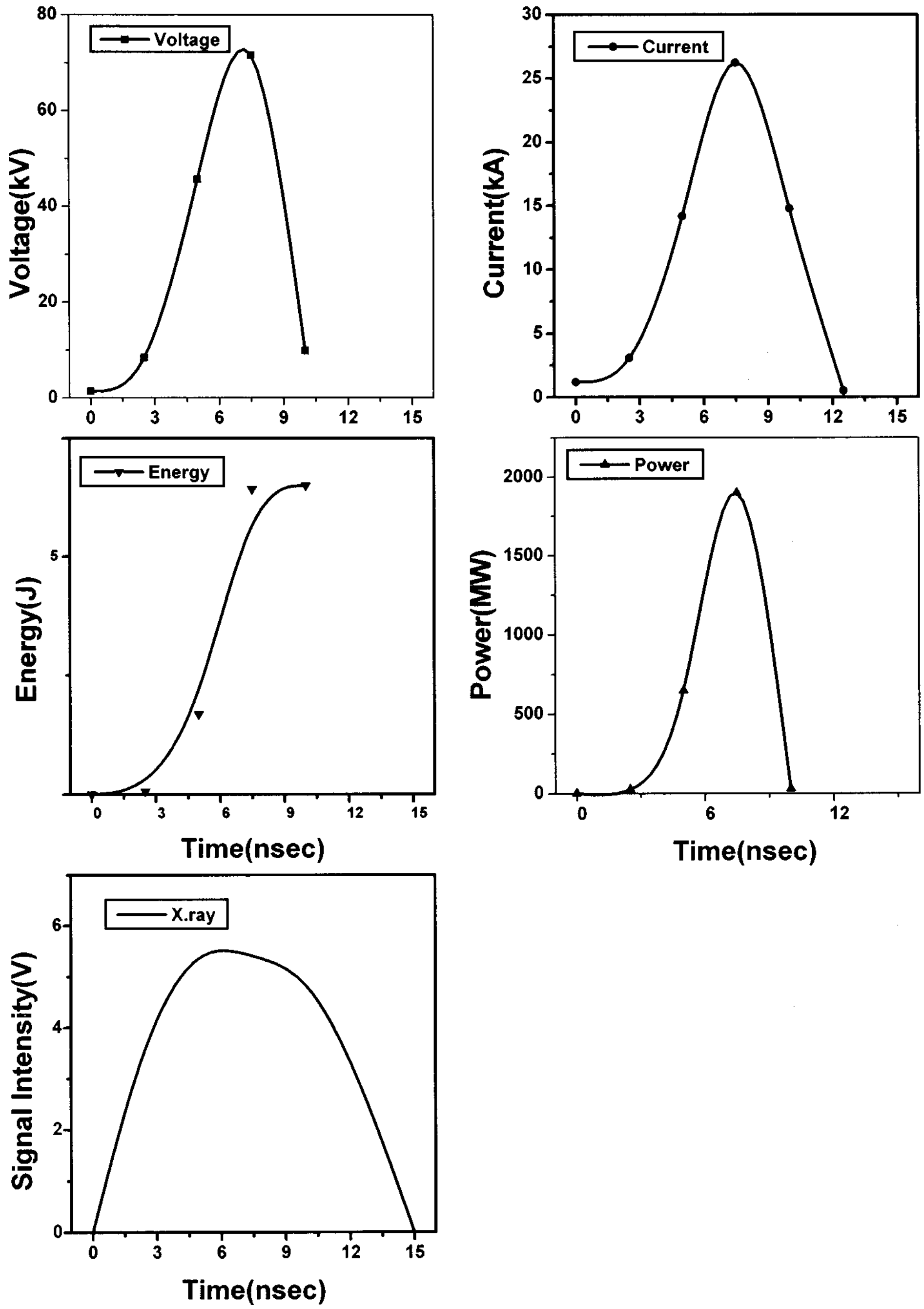

FIG. 5. Temporal variation of voltage, current, energy, and power across the diode, and temporal x-ray emission wave form detected by the *p-i-n* diode.

with the latter two targets, but not with the former ones. Figure 4 contains the variation in impedance with change in electrode separation, and temporal variation of diode impedance for different separations between anode and cathode, which are suitable for x-ray generation. Figure 5 shows the variation of voltage, current, power, energy, and x-ray emission as recorded by the *p-i-n* diode masked with the earlier mentioned filter, for 1.3 mm separation between the diode electrodes. The data for both figures is taken with the lead target.

The x-ray emission by impact of a 70 keV electron beam from titanium, copper, molybdenum, tin, tantalum, and lead is calculated,[9] and the results are presented in Fig. 6. The Ross filters may help us to analyze whether the observed x rays are essentially continuum radiation, or the line radiation, characteristic of the target. It is found that in the case of molybdenum target, the emitted radiation has a significant contribution of K_α, whereas for tantalum and lead targets the radiation are dominantly continuum. A lower but significant contribution of line radiation is expected from the tin target.

IV. DISCUSSION AND CONCLUSION

The experiment is performed at fixed charging voltage of 30 kV. The voltage which appears across the diode, is measured at 70±10 kV. On varying the separation between the diode electrodes from 1.3 to 1.8 mm, the diode impedance,

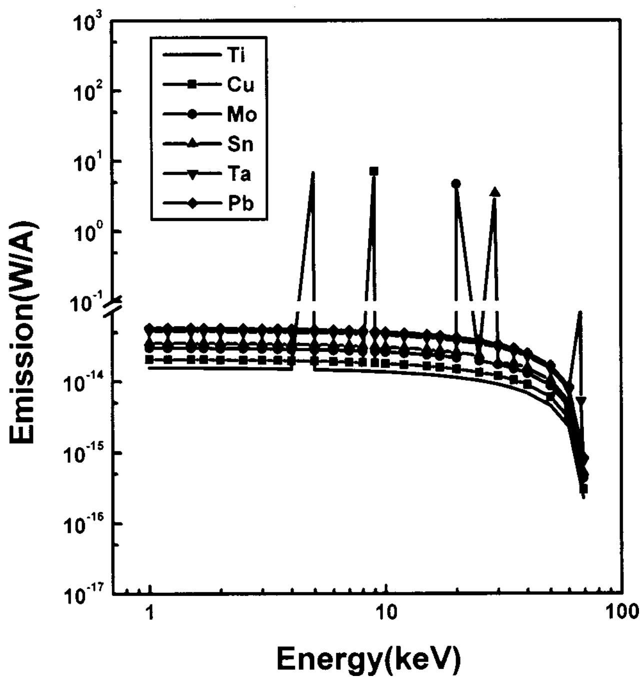

FIG. 6. X-ray emission spectrum (calculated) from different material anodes by impact of 70 keV electron beam.

measured as the ratio of voltage to current, changes between 2.7 to 3 Ω. With further increase in distance to 2.0 mm, the x-ray emission ceases, although the high voltage (HV) probe shows about 88 kV appearing across the diode. Probably, the increase in diode impedance delays the discharge, and the increased voltage gives way to a discharge along the chamber wall which takes away the energy.

The x-ray emission from thick targets by impact of an electron beam is thoroughly investigated by several workers. Dyson[10] concentrated on a range of electron energies between 9 and 15 kV. Green,[11] Green and Cosslett[12] studied the efficiency of continuous x-ray production by impact of up to 50 keV electrons. Metchnik and Tomlin[13] extended the investigation up to 70 keV electrons. Thordarson,[14] and Sesemann[15] used a 60–170 keV electron beam. The subject is extensively reviewed by Dyson.[9] The x-ray emission is reported minimum along the target surface, when the electron beam is incident perpendicular to the target. The emission attains an appreciable value at 20° with respect to the target surface, and does not change much for higher angles. In this experiment, the inclination angles of different detectors, that is, the PMT, *p-i-n*-diode, and DEF with respect to the target remained at 40°–60°, as the positioning at different angles was not possible without changing the vacuum chamber. The detectors' position was fixed during the experiment for low to high *Z* targets. In the case of low *Z* targets, that is, titanium and copper, the x rays could not be recorded efficiently on DEF. The PMT signal is weak and shot to shot variation significant. This is not surprising, as x-ray emission intensity is approximately proportional to *Z* (for example, see Ref. 9). Since the detectors are placed outside the experimental chamber, the generated x-ray flux after passing through the chamber wall may not remain significant at the detectors. For the molybdenum target, the x-ray emission is found quite reproducible. The reproducibility increases steadily with increase in *Z* of the target and is found very reproducible for lead. The x-ray signal intensity does not increase much with *Z*. This is because the absorption of x-ray photons within the target increases also with the increase in target atomic number. It is reported that[10–12] the efficiency of continuous x-ray production decreases with *Z* to about $Z=50$, and then increases again. As expected, the x radiation from the molybdenum target has a significant contribution from K_α, but tantalum and lead targets emit essentially continuum radiation. Tothill[16] reported the variation in ratio of characteristic K_α to continuum radiation for copper and tungston targets. For copper, a maximum of about 0.75 is observed at 40 kV, and then the ratio decreases again with increase in accelerating potential. For tungston, above 70 kV, the ratio starts to increase and saturates to below 0.1 at about 250 kV. He also extrapolated this ratio for different element targets, assuming the ratio of electron beam energy to K_α energy (U) fixed at 2. Tothill's extrapolation suggested the ratio 26% for Mo target, 2.2% for Ta target, and 0.8% for Pb target. In this experiment, the ratio of K_α to continuum for Mo target is found 17%±10%, whereas no conclusion about the ratio for Ta and Pb could be drawn. The mismatch with the Tothell's extrapolation may not be surprising. In this experiment, $U=3.5$ for Mo target. Thus, in the present measurement, a significant contribution of characteristics radiation from molybdenum, and continuum x-radiation emission from tantalum and lead targets are in agreement with the previously reported results.

It may be of interest to compare the CERES with other pulsed x-ray sources like x pinch, vacuum spark, *Z* pinches, and plasma focus. The CERES is operated at input discharge energy of just 30 J, an order of magnitude smaller than above mentioned low energy devices developed so far. But the shot-to-shot reproducibility for x-ray emission is much better. The x-ray pulse width (FWHM) from CERES (10±1 ns) is much wider than x pinch (∼1 ns),[17] of the same order as wire array *Z* pinch,[18] and narrower than plasma focus (30–50 ns).[19]

In conclusion, an x-ray diode energized by a low energy Blumlein is studied, which may be used as characteristics or continuum radiation source of choice, and may find applications in different disciplines like radiography, crystallography, x-ray contact microscopy and x-ray backlighting.

ACKNOWLEDGMENTS

This work was conducted at The Blackett Laboratory, Imperial College London. One of us (Dr. M. Zakaullah) acknowledges the support of Commonwealth Scholarship Commission, for financial support during stay and work at Imperial College London. The authors acknowledge useful discussion with Professor A. E. Dangor.

[1] D. H. Kalantar, D. A. Hammer, A. E. Dangor, J. M. Bayley, and F. N. Beg, AIP Conf. Proc. **299**, 191 (1993).
[2] A. Ikhlef and M. Skowronek, AIP Conf. Proc. **299**, 218 (1993).
[3] V. L. Kantsyrev, K. I. Kopytok, and A. S. Shlyaptseva, AIP Conf. Proc. **299**, 226 (1993).
[4] P. Lee, X. Feng, G. X. Zhang, M. H. Liu, and S. Lee, Plasma Sources Sci. Technol. **6**, 343 (1997).

[5] K. Bergmann, R. Lebert, and W. Neff, J. Phys. D: Appl. Phys. **30**, 990 (1997).
[6] D. N. Chesney and M. O. Chesney, *X-ray Equipment for Student Radiographers* (Blackwell Scientific, Oxford, 1987), p. 101.
[7] R. Coisson, in *Imaging Processes and Coherence in Physics*, edited by M. Schlinker, M. Fink, J. P. Geodgebuer, C. Malgrange, J. Ch. Vienot, and R. H. Wade (Springer, Berlin, 1980), p. 51.
[8] J. P. VanDevender, Ph.D. thesis, Imperial College London, 1974.
[9] N. A. Dysan, *X-Rays in Atomic and Nuclear Physics* (Cambridge University Press, Cambridge, 1990), p. 7.
[10] N. A. Dyson, Br. J. Appl. Phys. **10**, 505 (1959).
[11] M. Green, Proc. Phys. Soc. London **83**, 435 (1964).
[12] M. Green and V. E. Cosslett, J. Phys. D: Appl. Phys. **1**, 425 (1968).
[13] V. Metchnik and S. G. Tomlin, J. Phys. D: Appl. Phys. **1**, 1093 (1963).
[14] S. Thordarson, Ann der Phys. **35**, 135 (1939).
[15] G. Sesemann, Ann der Phys. **40**, 66 (1941).
[16] P. Tothill, J. Phys. D: Appl. Phys. **2**, 1093 (1968).
[17] T. A. Shelkovenko, S. A. Pikuz, D. A. Hammer, Y. S. Dimant, and A. R. Mingaleev, Phys. Plasmas **7**, 2840 (1999).
[18] T. W. L. Sanford *et al.*, Phys. Plasmas **6**, 2030 (1999).
[19] M. Zakaullah, I. Akhter, A. Waheed, K. Alamgir, A. Z. Shah, and G. Murtaza, Plasma Sources Sci. Technol. **7**, 206 (1998).